

Supporting Information

High-efficient Fluorescent and Magnetic Multi-Modality Probes for Long-Term Monitoring and Deep Penetrating Imaging of Tumor

Lingchen Meng^{‡a}, Xibo Ma^{‡b,c}, Shan Jiang^a, Guang Ji^a, Wenkun Han^a, Bin Xu^a, Jie Tian^{*b,c}, Wenjing Tian^{*a}

^aState Key Laboratory of Supramolecular Structure and Materials, Jilin University, Changchun, 130012, P. R. China

^bKey Laboratory of Molecular Imaging, Institute of Automation, Chinese Academy of Sciences, Beijing, 100190, P. R. China

^cThe University of Chinese Academy of Sciences, Beijing, 100049, China.

E-mail: wjtian@jlu.edu.cn

Experimental Section

1. Materials

All reagents and starting materials are commercially available and were used without further purification, unless otherwise noted. 4-Bromophenylacetonitrile, Iodine, Sodium methylate solution (30 wt% in methanol (ca. 5mol/L in Methanol)), $\text{Ph}_3\text{P}^+\text{CH}_3\text{Br}^-$, *t*-BuOK, 4-(Diphenylamino) benzaldehyde, $\text{Pd}(\text{OAc})_2$, AgCO_3 and Tetrahydrofuran (THF) were purchased from Aladdin (Shanghai, China). Diethyl ether and Toluene were purchased from Titan Scientific Co.,Ltd (Shanghai, China). Ferric acetylacetonate, Benzyl ether and Oleylamine was purchased from Tokyo Chemical Industry Co., Ltd. (Shanghai). Polystyrene-poly (ethylene glycol) (PS-PEG) were purchased from Sigma-Aldrich. Deionized water (18.2 M Ω cm resistivity) from a Milli-Q water system was used throughout the experiments before being used as solvents.

2. Instrumentations

^1H NMR spectra were recorded on Bruker AVANCEIII 500 MHz spectrometer with tetramethylsilane as the internal standard. Mass spectra were recorded on a Bruker autoflex speed TOF. The self-assembly process was completed using a bath sonicator (Bransonic, MH 2510). UV-vis absorption spectra were recorded using a SPECORD 210 PLUS UV-vis spectrophotometer. Fluorescence spectra were recorded by Shimadzu RF-5301 PC spectrometer and Maya2000Pro optical fiber spectrophotometer. Transmission electron microscopy (TEM) images were obtained using a transmission electron microscope (TEM, JEM-2100F). Scanning electron microscope (SEM) images were obtained on a HITACHI SU8020 SEM. The FTIR spectra were measured by a Fourier Transform Infrared Spectrometer (FTIR) (Bruker, VERTEX 80V). DLS measurement was performed using a Malvern Zetasizer Nano ZS size analyser at room temperature. Magnetization curves were obtained from SPIO and TSP NPs using a Quantum Design MPMS-XL-7 superconducting quantum interference device (SQUID) magnetom (Quantum Design, SanDiego,CA). Fluorescence lifetime measurements were performed on a fluorescence lifetime platform from Edinburgh FLS980.

3. Synthesis of 2-(4-bromophenyl)-3-(4-(4-(diphenylamino)styryl) phenyl)

TB was synthesized according to the literature. ^[1] 2,3-bis(4-bromophenyl) fumaronitrile and 4-(Diphenylamino) styrene were prepared according to the method described in ref. ^[1]. 2,3-bis(4-bromophenyl) fumaronitrile (200 mg, 0.52 mmol), 4-(Diphenylamino) styrene (140 mg, 0.52 mmol), $\text{Pd}(\text{OAc})_2$ (6 mg, 0.026 mmol), and Ag_2CO_3 (85 mg, 0.31 mmol) were dissolved in toluene (10 mL) at a 50 mL Schlenk tube. The reaction solution was further stirred at 110 °C for 18 h. The resulting solution was filtered to isolate the solid, which was rinsed with DCM. After the evaporation of solvents, the crude product was purified by silica gel column chromatography using DCM/ *n*-hexane in the volume ratio of 2:1 as eluent. TB was obtained as a red solid in 62.8% yield. ^1H NMR (500 MHz, DMSO) δ 7.82 (ddd, *J* = 13.8, 8.6, 6.0 Hz, 8H), 7.55 (d, *J* = 8.7 Hz, 2H), 7.43 (s, 1H), 7.39 (s, 1H), 7.33 (dd, *J* = 8.3, 7.5 Hz, 4H), 7.22 (s, 1H), 7.19 (s, 1H), 7.11-7.03 (m, 6H), 6.96 (d, *J* = 8.6 Hz, 2H).

4. Synthesis of Superparamagnetic iron oxide (SPIO)

SPIO was obtained via a method reported previously. ^[2] $\text{Fe}(\text{acac})_3$ (6mmol) was dissolved in 20 mL of benzyl ether and 40 mL of oleylamine. The solution was dehydrated at 110 °C for 1 h under N_2 atmosphere, then quickly heated to 300 °C at a heating rate of 20 °C/min and aged at this temperature for 1 h. After the reaction, the solution was allowed to cool down to room

temperature. The Fe₃O₄ NPs were extracted upon the addition of 50 mL of ethanol, followed by centrifuging. The Fe₃O₄ NPs (yield ~ 800 mg) were dispersed in nonpolar solvents such as hexane and toluene.

5. Preparation of TB/SPIO@PS-PEG nanoparticles (TSP NPs)

In a typical preparation, the fluorescent TB, SPIO, PS-PEG were respectively dissolved in THF to make a 1 mg mL⁻¹, 1 mg mL⁻¹, 5 mg mL⁻¹ stock solution. 50μL TB(1 mg mL⁻¹) , 50μL SPIO(1 mg mL⁻¹) and 100μl PS-PEG (5mg mL⁻¹) were dispersed in 1mL THF by a vigorous bath sonicator. The solution mixture was quickly added to DI water, and the THF was removed by nitrogen stripping in a vigorous bath sonicator. The solution was concentrated by continuous nitrogen on a 90 °C hotplate followed by filtration through a 0.2-micron filter. During nanoparticle formation, the TB and SPIO tended to entangle with the hydrophobic domains of PS-PEG, to afford the hydrophobic interiors, while the hydrophilic domains of PS-PEG extend into the aqueous phase of the NPs.

6. Determination of quantum yields

By using Rhodamine B as the reference (fluorescence quantum yield equal to 0.69 in dilute ethanol solution with excitation wavelength of 365 nm), the fluorescence quantum yield of the near-infrared emission dots were measured according to the following equation.

$$\Phi_s = \Phi_r \left(\frac{A_r}{A_s} \right) \left(\frac{I_s}{I_r} \right) \left(\frac{n_s}{n_r} \right)^2$$

where Φ_r is the quantum yield of reference. A_r is the absorbance of reference at the excitation wavelength. A_s is the absorbance of sample at the excitation wavelength. I_r is the area under the emission peak on a wavelength scale of reference. I_s is the area under the emission peak on a wavelength scale of sample. n_r is the refractive index of the reference solvent, n_s is the refractive index of the sample solvent. Absorption spectrum and emission spectrum measured by the Maya 2000 pro fiber spectrometer (Ocean Optics). Solid state PL efficiencies were measured by using an integrating sphere (C-701, Labsphere Inc.) with a 365 nm Ocean Optics LLS-LED as the excitation source, and the laser was introduced into the sphere through the optical fiber.

7. Molecular dynamics simulations

Molecules for molecular dynamics (MD) simulations were generated by GaussView 5.0.8 (Gaussian, Inc., Wallingford, CT). MD simulations of systems containing pure TB, pure SPIO, pure PEG, pure PS and mixed TB-SPIO, mixed TB-PEG, mixed TB-PS were performed to obtain target microstructures. For TB-SPIO blends, 40 SPIO models (every SPIO was built by 20 units) and 4 TB have been put randomly in a large unit cell (50Å * 50Å * 50Å). For TB-PEG blends, 40 PEG models (every PEG was built by 20 units) and 4 TB have been put randomly in a large unit cell (50Å * 50Å * 50Å). For TB-PS blends, 40 PS models (every PS was built by 20 units) and 4 TB have been put randomly in a large unit cell (50Å * 50Å * 50Å). According to the Flory–Huggins solution theory, ΔG_{mix} and χ follow the relation

$$\frac{\Delta G_{mix}}{RT} = n_1 \ln \phi_1 + n_2 \ln \phi_2 + n_1 \phi_2 \chi$$

, where n_1 is the number of moles of TB, n_2 is the number of moles of polymer or SPIO, ϕ_1 and ϕ_2 are the volume fractions of the two components in the blend, R is the ideal gas constant and T is the absolute temperature. The enthalpy of mixing $\Delta H = [H_{blend} - H_1 - H_2]$ can be deduced from MD simulations on the blend and pure components to determine H_{blend} , H_1 and H_2 , respectively. CompassII force fields were used. (i) An initial NPT simulation was performed at room temperature while keeping the density low (~1 g/cm³)

for 500ps, (ii) 5 successive 500ps -molecular dynamics (NPT, $p = 1 \text{ atm}$) were then performed; (iii) finally, a 20ps molecular dynamics (NPT; $p = 1 \text{ atm}$, $T = 298 \text{ K}$) was performed and snapshots saved every 1ps for further analysis.

8. Cell imaging and Cell viability analysis

To study the cellular uptake, Huh-7 cells were added to 6-well plate. The TSP NPs and Hoechst33258 were incubated with Huh-7 cells for 6 h at a concentration of 20mg/mL, and the fluorescence was monitored by laser confocal fluorescence microscope (CLSM). The cytotoxicity of TSP NPs towards Huh-7 cells were evaluated by following the instructions of MTS cell proliferation colorimetric assay kit. 5000 cells/well in a 100 μL suspension were incubated in 96-well plates for 24 h. Then, 100 μL fresh culture medium containing TSP NPs with various concentrations (1 $\mu\text{g/mL}$, 2 $\mu\text{g/mL}$, 5 $\mu\text{g/mL}$, 10 $\mu\text{g/mL}$, and 20 $\mu\text{g/mL}$) were added into each well. After incubation for 24h and 48h, the culture medium was removed, and the cell well was washed three times with PBS. In the end, 100 μL of MTS reagent was added to each well and incubated for 2 h under 5% CO_2 at 37°C. The absorbance at 450 nm was measured, using a microplate, by absorbance reader (Bioradi MARK, USA).

9. Ethics statement

This study was performed with the approval of the Experimental Animal Manage Committee (EAMC) of Perking University. Animals were treated as the guidelines of EAMC.

10. Animal experiments

The nude mice (5 weeks, male) were obtained from the Beijing Vital River Laboratory Animal Technology Co., Ltd. Two types of tumor models were established: subcutaneous tumor and orthotopic tumor. Briefly, Huh-7 cells were incubated with 20 $\mu\text{g/mL}$ TSP NPs incubated for 6 h at 37 °C. 200 μL of PBS (0.01 mol/L, pH 7.2) containing a suspension of $\sim 4 \times 10^4$ Huh-7 labelled cells were subcutaneously injected into the right-side leg and $\sim 10^6$ Huh-7 labelled cells were subcutaneously injected abdomen to form different subcutaneous tumor model mouse. And the tumor model in situ was built next. Surgical site at abdomen was cleaned and a midline incision was made in the abdomen to expose the left lobe of liver. The cell suspension of $\sim 10^5$ Huh-7 labelled cells was directly injected into the parenchymal cells of the liver. Abdomen was then sutured with maxon (monofilament polyglyconate synthetic absorbable suture) and skin closed with prolene (polypropylene suture). Mice were kept warm after the surgery and returned to their cages when fully awake.

11. In vivo fluorescence imaging

The subcutaneous tumor model mice were imaged using an IVIS Spectrum Imaging System (Xenogen Co., Alameda, CA, USA) while under anesthesia using 1%–2% of isoflurane in oxygen. The fluorescence images were recorded with 1s exposure using a filter 660 nm upon excitation at 465 nm. The autofluorescence was removed using the software of IVIS Spectrum Imaging System. The time-dependent fluorescence intensity of regions of interest (ROI) in the tumor was recorded with a 1 s exposure upon excitation at 465 nm and emission at 660 nm. Scans were carried out on days 0, 1, 3, 7, 12, 18 and 24. After designated time intervals postsurgical operation, the orthotopic tumor model mice was imaged using the TomoFluo3D optical imager. Planar pictures of fluorescence (excitation at 480 nm and emission at 650 nm, 5s exposure time) were taken at various time from 0day to 10day. 3D scans were done on the tumor zone after 10 days.

12. Magnetic resonance imaging (MRI) study in vivo and ex vivo

All experiments were conducted on a 1 T magnet (Aspect, Oxford, UK) equipped with a 60-mm inner diameter gradient coil. The maximum strength of the gradient coil was 1500 mT/m⁻¹, with a rise time of 100 ms. Images were acquired using a home-built mouse head cage coil. Mice were positioned on a custom-made mouse cradle and anesthetized with 2% isoflurane in O₂ mixture with total flow rate of 1,200 mL•min⁻¹. T₂-weighted RARE MRI were acquired using the following parameters: TR, 55 ms; TE, 5000ms; slice thickness, 2.0mm; slice spacing, 0.2 mm; matrix 224×192; FOV 10 cm×10 cm.

13. Magnetic particle imaging (MPI) imaging study in vivo and ex vivo

All MPI studies in this work are performed on a 3D MPI scanner (Magnetic Insight Inc, MOMENTUM™ Imager). The frequency of MPI is 45 kHz; The magnetic gradient strength of MPI is 6T/m. The original dates were processed by VivoQuant software. CT imaging was conducted using Optical Multimodality Molecular Imaging System for Small Animal under voltage of 45 kV, electricity of 0.8 mA. MPI images were reconstructed using a VivoQuant software.

Supporting Figs

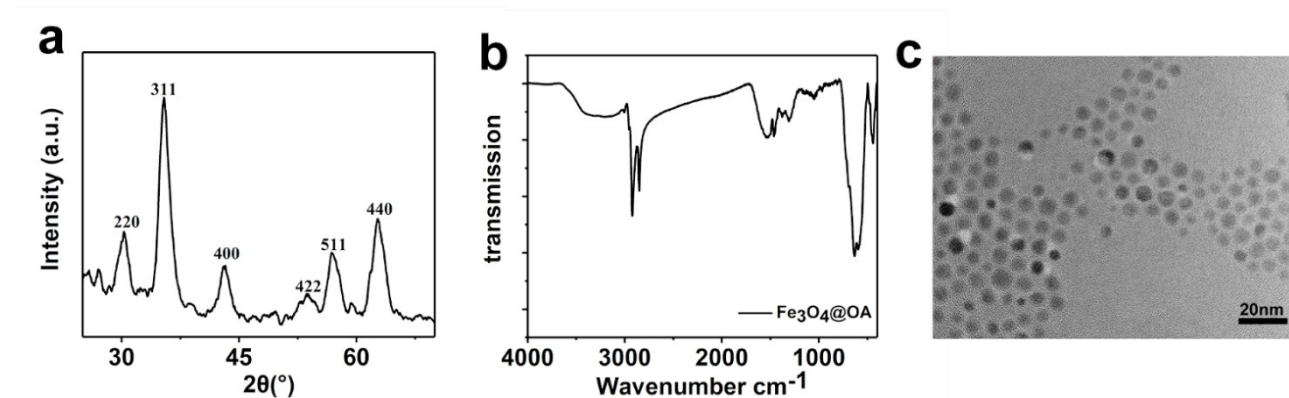


Figure S1 (a) XRD pattern of SPIO. (b) FTIR spectrum of SPIO. (c) TEM image of the SPIO

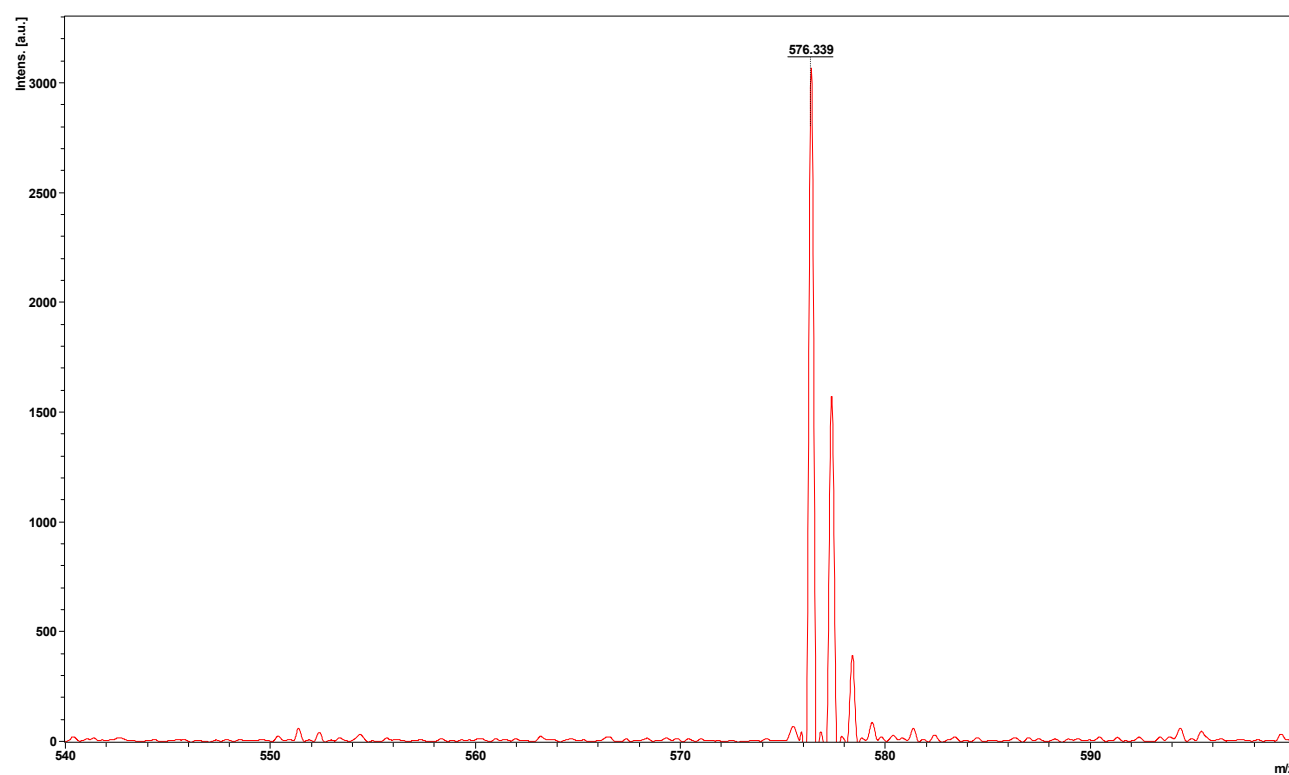


Figure S2 HRMS (MALDI-TOF) spectrum of TB

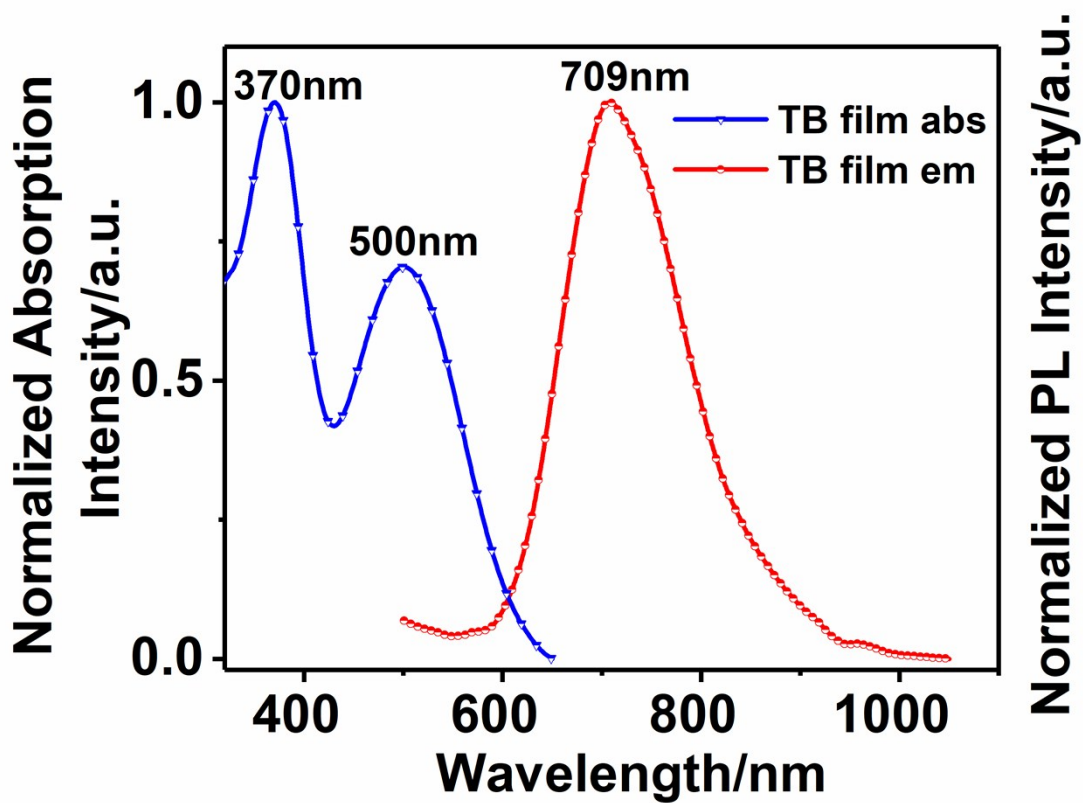


Figure S3 Normalized UV-vis absorption and PL emission spectra of TB in film.

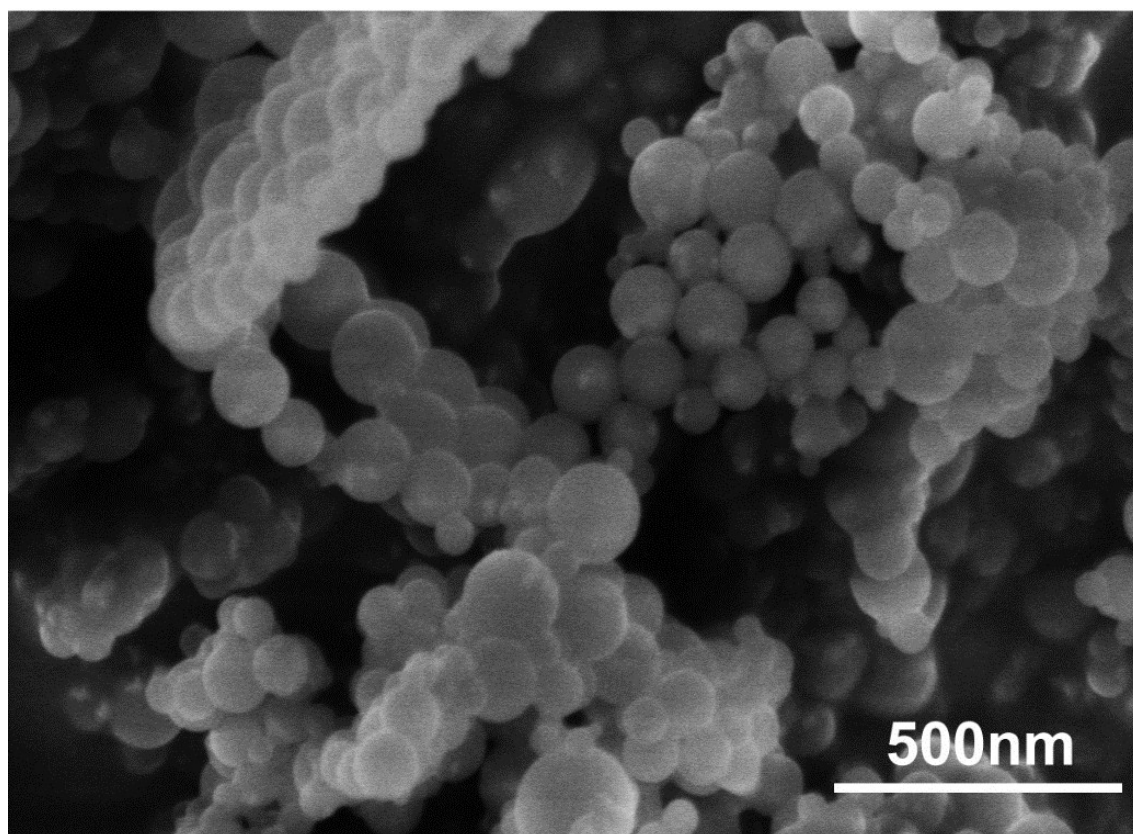


Figure S4 SEM images of TSP NPs

Table S1 Summary of photophysical properties of TS NPs, TSP NPs, and TP NPs.

	λ_{em} (nm)	QYs (%)	τ (ns)	k_r (ns ⁻¹)	k_{nr} (ns ⁻¹)
TS	709	0.9587	1.87	1.60	5.19
TSP NPs	655	14.6	4.02	3.37	2.15
TP NPs	652	16.53	4.24	4.49	1.91

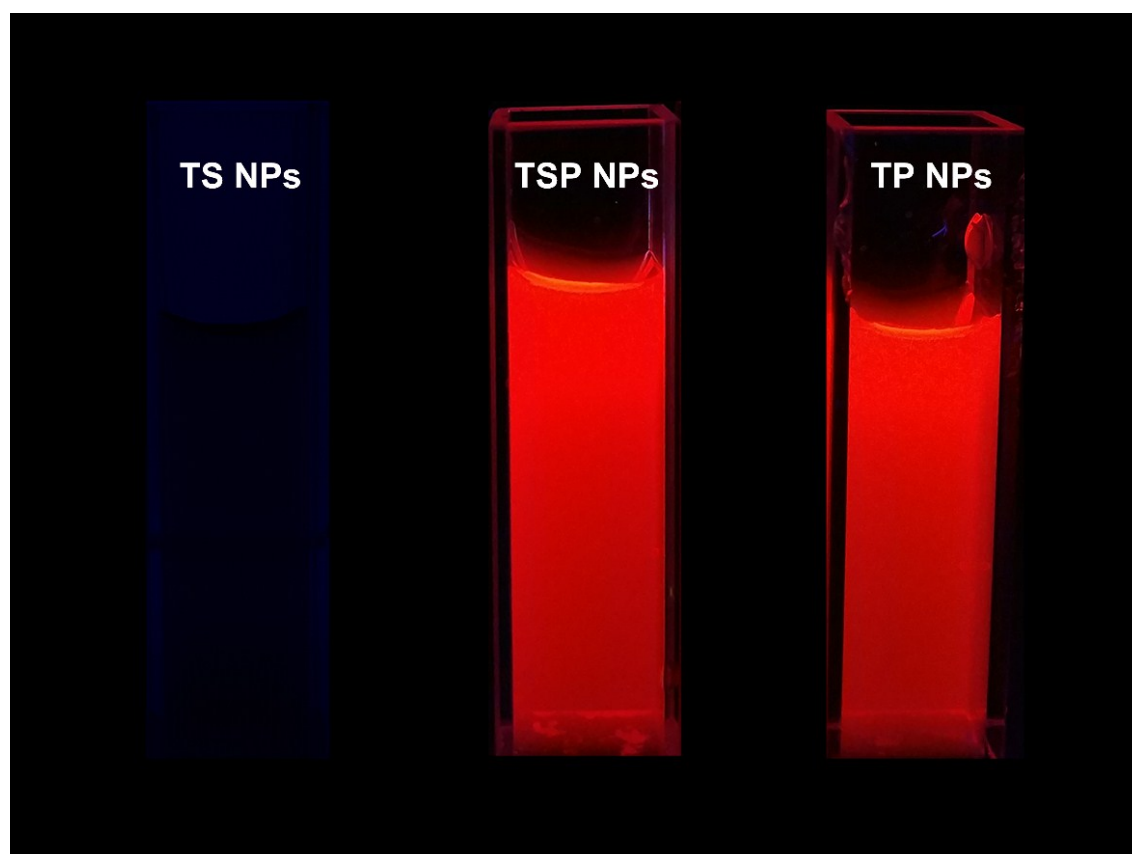


Figure S5 Photographs of water solutions of TS NPs, TSP NPs and TP NPs taken under 365 nm UV illumination.

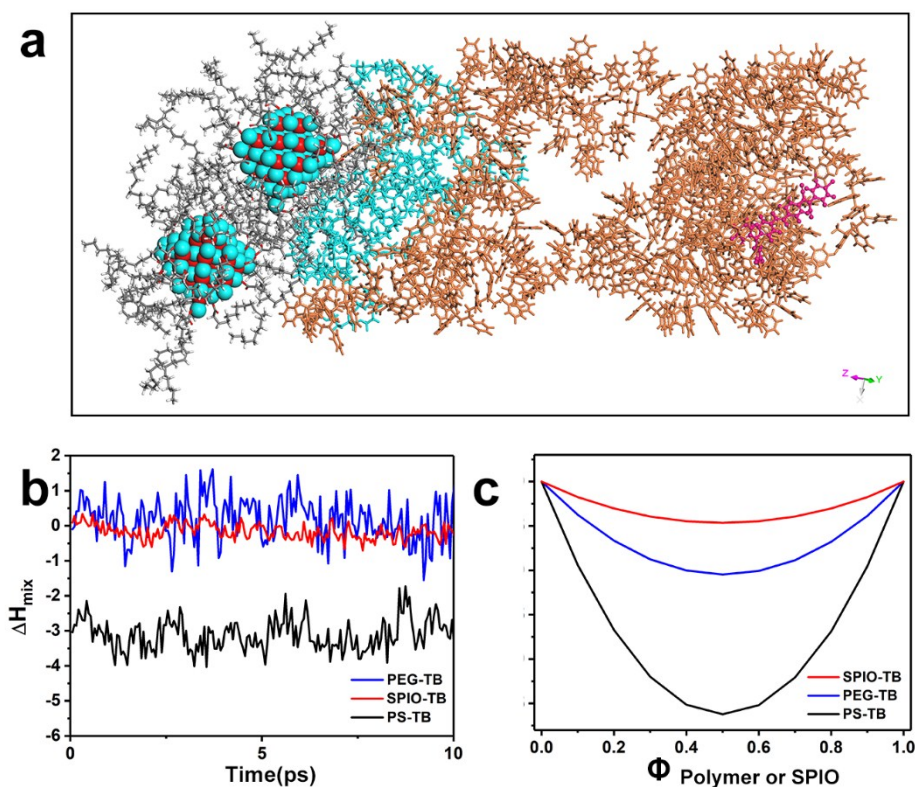


Figure S6 (a) Molecular dynamics (MD) simulations of the mixing of TB, SPIO and PS-PEG. (b) The enthalpy of mixing of TB blend with SPIO (SPIO-TB) (red line), Polyethylene glycol (PEG) (PEG-TB) (blue line), Polystyrene (PS) (PS-TB) (black line). (c) The change in free energy of mixing as a function of volume fraction polymer for the SPIO-TB, PEG-TB, PS-TB system as predicted using Flory-Huggins lattice theory with different values of the interaction parameter.

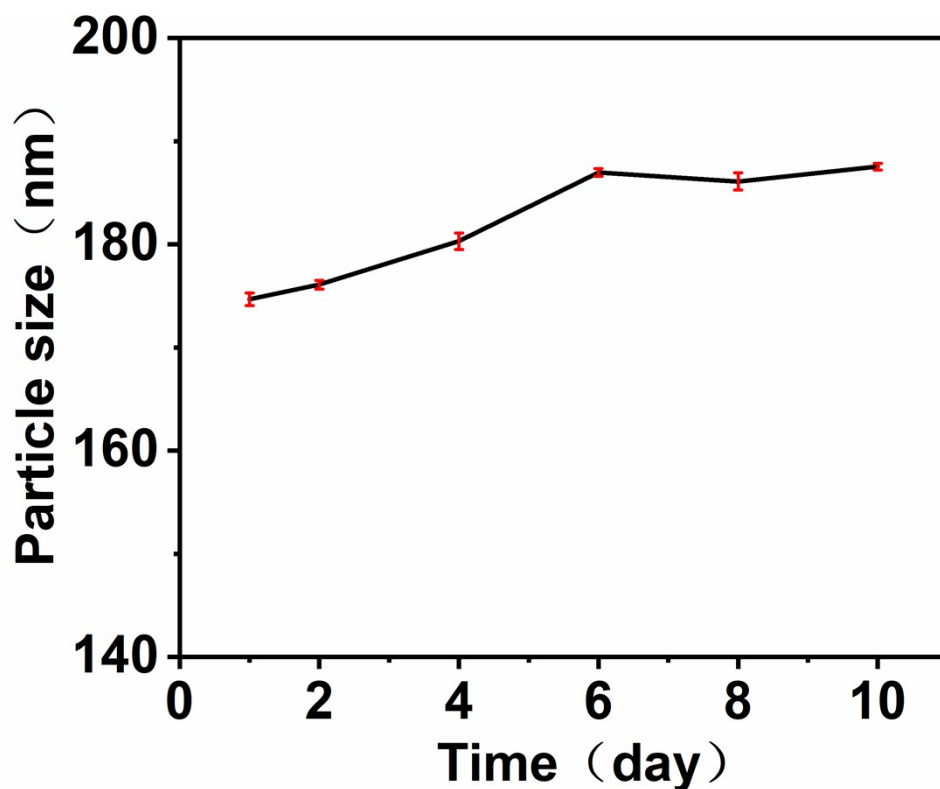


Figure S7 Colloidal stability assay via dynamic light scattering measurements of TSP NPs stored in FBS solution at 37°C for 0, 2, 4, 6, 8, 10 days.

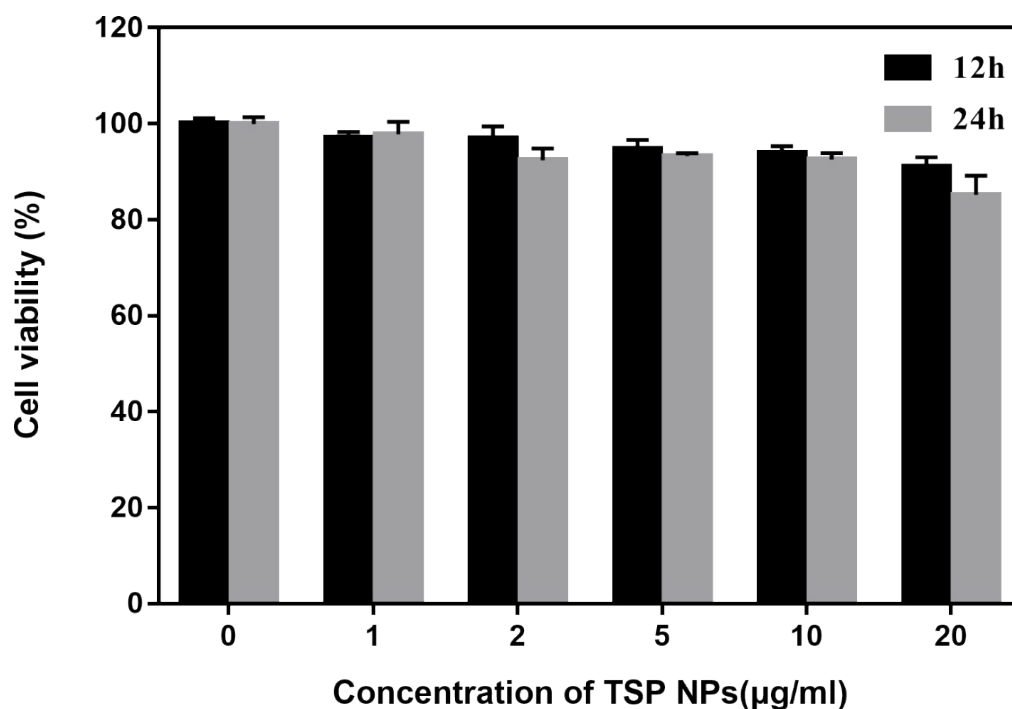


Figure S8 Viability of Huh-7 cancer cells incubated with TSP NPs at various concentrations after 12 h and 24h.

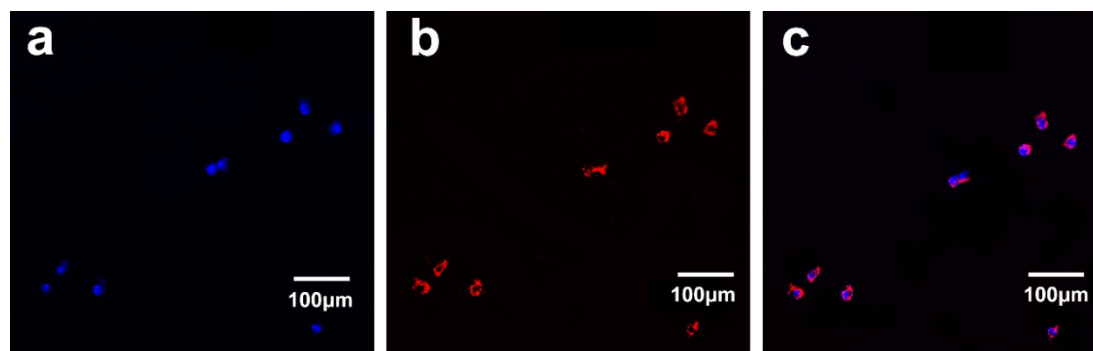


Figure S9 Confocal microscopy images of Huh-7 cells stained with Hoechst33258 and TSP NPs (a) Channel blue: fluorescent nucleus imaging stained with Hoechst33258, excitation wavelength: 405 nm, scan range: 425–490 nm; (b) Channel red: fluorescent cytoplasm imaging stained with nanoparticles, excitation wavelength: 488 nm, scan range: 600–700 nm; (c) Overlay imaging of a and b.

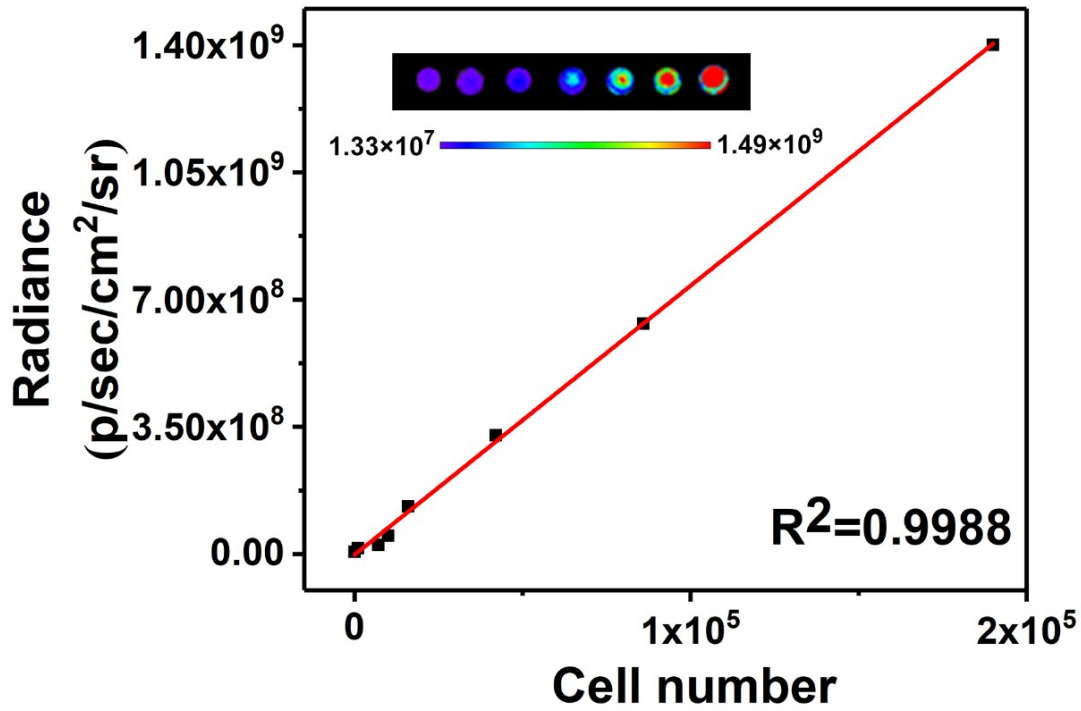


Figure S10 Plot of fluorescent signals versus the number of labeled cells ranging from 0–190 K (Insert is fluorescent image of well plates containing 1K–190 K cells)

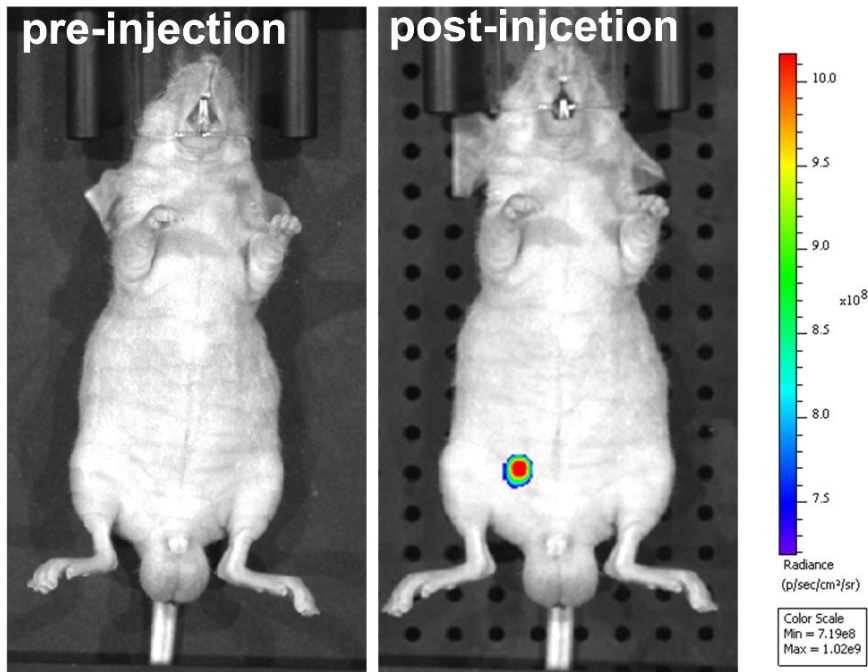


Figure S11 Representative in vivo fluorescence images of the nude mouse before and after subcutaneously injected with 1×10^6 of Huh-7 live cells

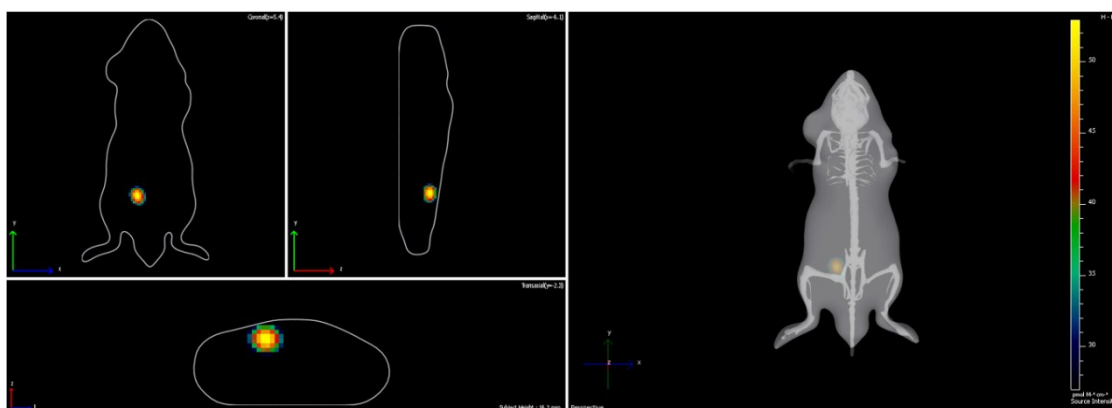


Figure S12 The 3D reconstruction fluorescence image of nude mouse after transplanted with 1×10^6 of HuH-7 cells labeled by TSP NPs for 1 h.

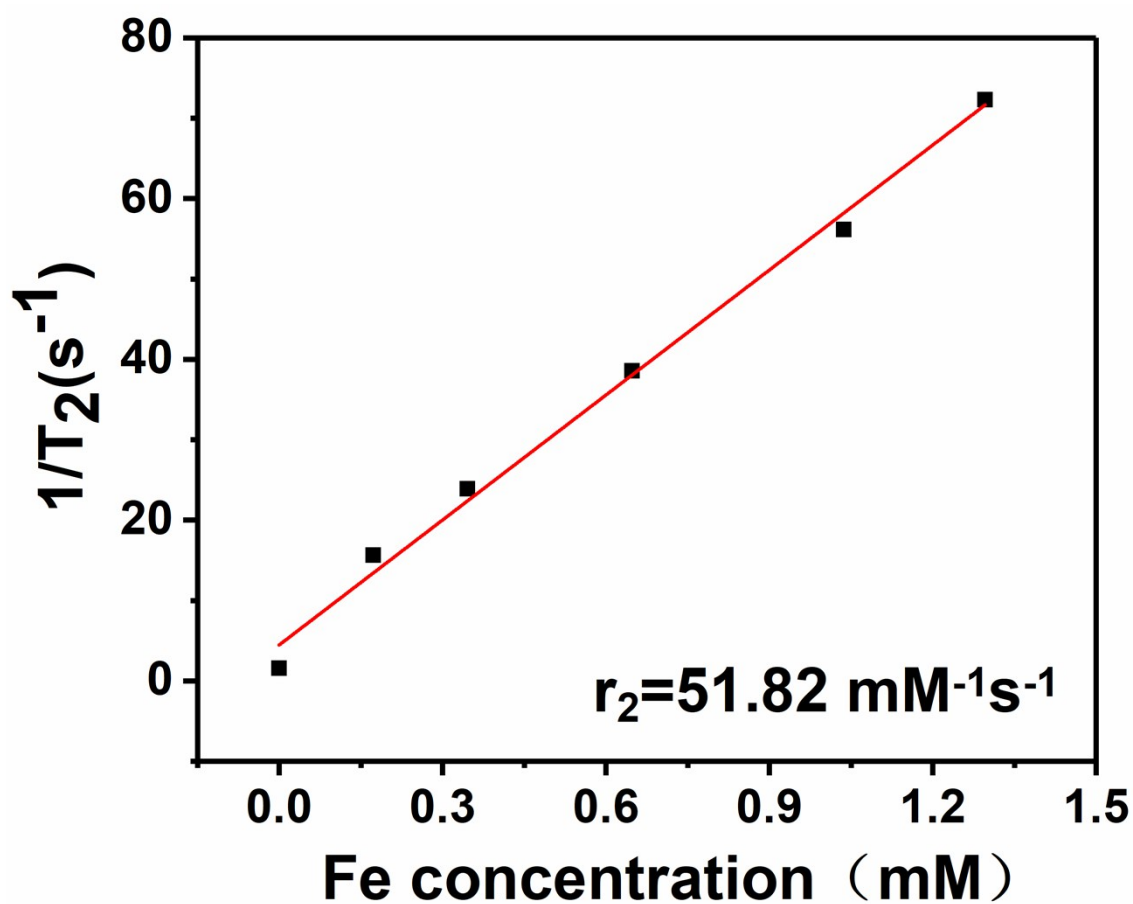


Figure S13 Plot of T_2 relaxation rate ($1/T_2$) for various iron concentrations (mM)

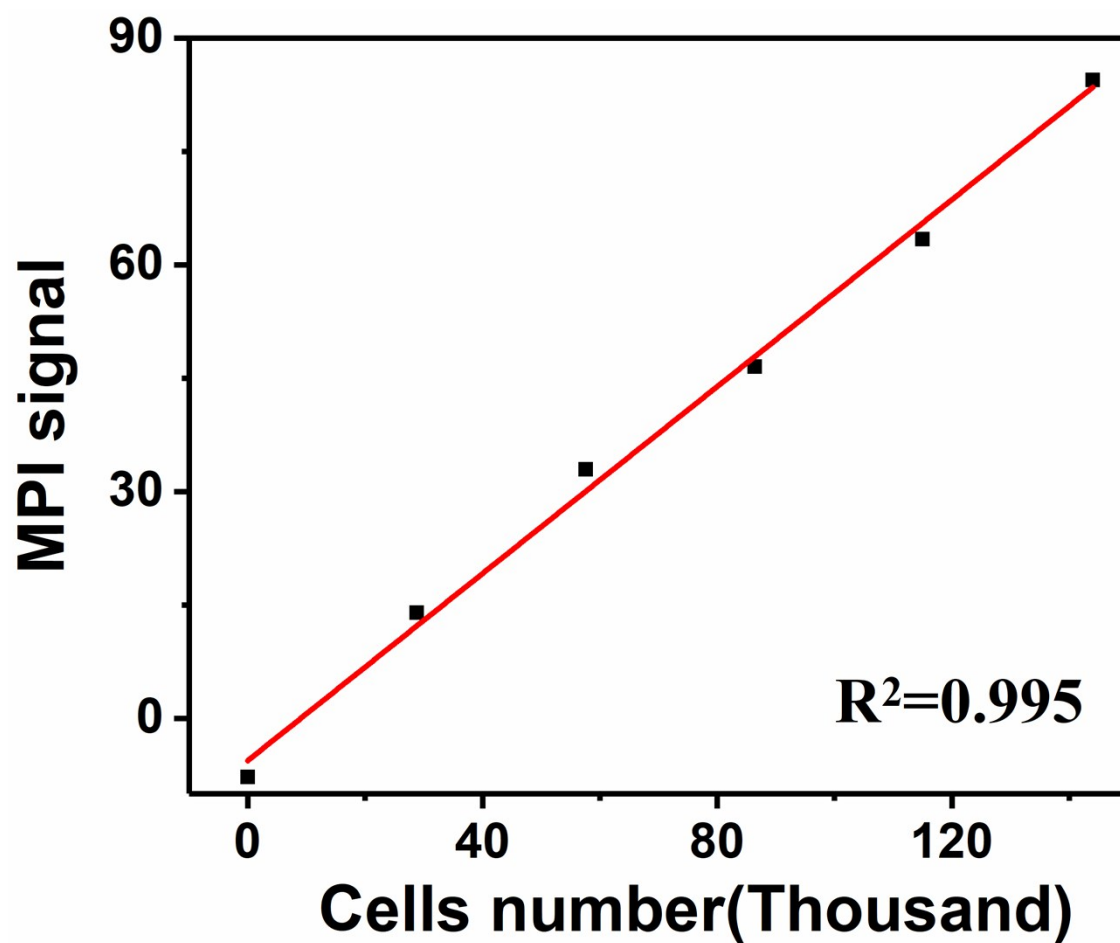


Figure S14 Plot of MPI signals versus the number of TSP NPs-labeled cells ranging from 0-144 K

Reference

1. N. Alifu, L. Yan, H. Zhang, A. Zebibula, Z. Zhu, W. Xi, A. W. Roe, B. Xu, W. Tian and J. Qian, *Dyes Pigments*, 2017, 143, 76-85.
2. Z. Xu, C. Shen, Y. Hou, H. Gao and S. Sun, *Chem Mater*, 2009, 21, 1778-1780.